Materials Science Forum
ISSN: 1662-9752, Vol. 1156, pp 27-35
doi:10.4028/p-F06BzD

Submitted: 2024-09-19
Revised: 2025-03-19
Accepted: 2025-03-19
Online: 2025-09-04

Lab-Based X-Ray Topography Characterization of Axial Samples from 4H-SiC Boules Grown by PVT Method

Yafei Liu[1,a*], Campbell Bouch[1,b], Pete Schunemann[1,c], Ryan Philpott[1,d], Mary Safko[1,e], Danielle Hamann[1,f], Mason Dupre[1,g] and Andrew Goldberg[1,h]

[1]Onsemi, 55 Executive Drive, Hudson, NH 03051, USA

[a]yafei.liu@onsemi.com, [b]campbell.bouch@onsemi.com, [c]pete.schunemann@onsemi.com, [d]ryan.philpott@onsemi.com, [e]mary.safko@onsemi.com, [f]danielle.hamann@onsemi.com, [g]mason.dupre@onsemi.com, [h]andrew.goldberg@onsemi.com

Keywords: SiC, PVT, Crystal Growth, Characterization, X-Ray Topography, Defects

Abstract. Axial sliced samples from 4H-SiC boules grown by PVT method were characterized by lab-based X-ray topography systems. Valuable information about dislocation behaviors during crystal growth was revealed. TSD/TMD propagation during PVT growth was studied. The different TSD/TMD propagation directions inside and outside the facet region were identified as the direct cause of the reduced TSD/TMD density at the facet boundary on some c-plane wafers. A defect reduction mechanism was proposed based on this discovery. It was observed that TSDs/TMDs were emitted by a void structure formed during crystal growth, which explained the elevated TSD/TMD density in the center regions of some wafers. The formation mechanism of such defect is different from the previous studies and remains under investigation.

Introduction

Technological developments in the past decade have driven demand for semiconductor devices that can meet the needs of high-power systems. Traditional silicon (Si)-based power electronic devices are reaching their performance limits. To address the demand of high-power systems, silicon carbide (SiC) materials have become one of the most promising semiconductor materials with their superior properties such as high saturation electron drift velocity, high thermal conductivity, and high breakdown electric field. As a result, SiC-based systems can achieve much lower losses and faster switching speed with smaller geometries than traditional Si-based systems. Commercially available SiC devices have been successfully adopted in many high temperature, high voltage, and high frequency applications. In recent years, the increased demand of electric vehicles has driven the adoption of SiC power electronic devices such as main traction inverters. Together with other applications for energy infrastructure and the most recent rising demand for data centers that are reliant on artificial intelligence (AI) technology, SiC systems have been giving benefits in a way of saving very large amounts of energy every day.

SiC devices have shown great success in industry. However, SiC materials quality is imperative to improving device yield, reducing the cost, and developing devices that can be used in higher power solutions. Currently, various defects exist in SiC materials grown by physical vapor transport (PVT), which is the most widely used method in industry. 0-dimensional defects include interstitial or substitutional atoms and vacancies. 1-dimensional defects refer to all kinds of dislocations including basal plane dislocations (BPDs), threading edge dislocations (TEDs), threading screw dislocations (TSDs), and threading mixed dislocations (TMDs). 2-dimentional defects are thin layers of stacking faults. 3-dimentional defects also exist such as voids and inclusions. Various characterization methods on crystalline defects are available including hot chemical etching, optical scans, electron microscopy, and X-ray topography (XRT) [1]. In this study, XRT is mainly used to non-destructively characterize the defects in 4H-SiC materials grown by PVT method.

The majority of XRT reported works were conducted at synchrotron facilities around the world [2-8]. However, the limited access to very few synchrotron sources is not able to meet the test requirements from daily research and production. In this study, Rigaku XRTMicron, a lab-based XRT system was used to characterize the defects in axial sliced samples from 4H-SiC boules grown by PVT method. XRT results were used to reveal the causes of distinct dislocation distribution in some c-plane SiC wafers.

Experiments and Methodology

Experimental PVT growth was conducted and some c-plane wafers with an off-cut angle of 4 degrees were cut, chemical mechanical polished (CMP) and characterized with XRT using 0008 reflection geometry on the Si side. Copper (Cu) target was used as the X-ray source and the $K\alpha_1$ radiation was selected and tuned by a special purpose multi-layer mirror for Cu target. TSD maps were generated by XRT Toolbox software, an automatic XRT data processing tool to generate defect analysis reports. Axial slices of PVT grown 4H-SiC boules were cut along $[11\bar{2}0]$ direction as shown in Fig. 1. Then the axial samples were fine ground on both sides down to the thickness of 500 μm. The axial samples were inspected by XRT using 0004 transmission geometry with molybdenum (Mo) $K\alpha_1$ radiation with another special purpose multi-layer mirror for Mo target. Topography images were enhanced in Fiji ImageJ software to observe defectivity.

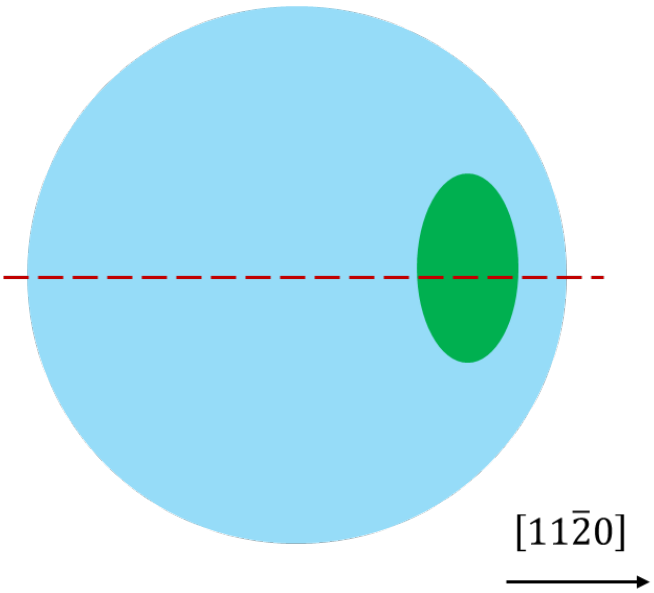

Fig. 1. Axial slice sample preparation from a PVT grown SiC boule.

Results and Discussions

Reduced TSD Density at the Facet Boundary. Fig. 2 shows a cropped TSD density map of a 150-mm c-plane 4H-SiC wafer. A reduced TSD density region is observed at the facet boundary marked by a red circle, which was identified by optical inspection of the different coloring effect from different nitrogen (N) doping. To investigate the cause of such TSD distribution, an axial sample prepared from another boule with the same growth process was inspected. Fig. 3 is a cropped overall XRT image of the axial sample. On the left side there are some contours because the lattice bending effect is giving some off-peak regions and the measurement recipe did not accommodate the change in this in-plane rotation. According to the $\boldsymbol{g} \cdot \boldsymbol{b}$ and $\boldsymbol{g} \cdot \boldsymbol{b} \times \boldsymbol{l}$ criteria [9], only TSDs or TMDs show strong contrast as linear features in the 0004 topography images. In some selected enlarged images shown in Fig. 4, dislocation behaviors that have been studied previously [10] such as replication from the seed, nucleation at the seed interface, deflection, climbing, and annihilation.

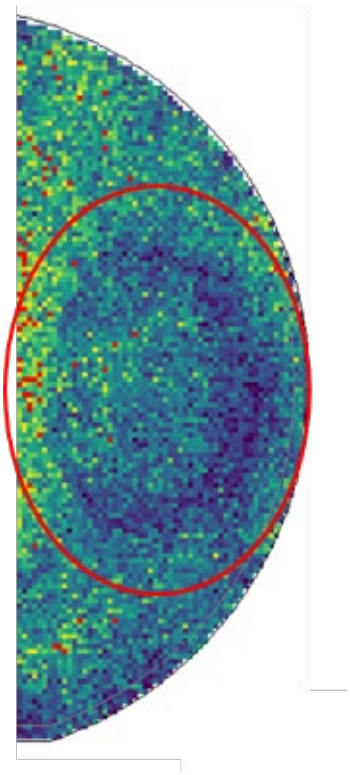

Fig. 2. A cropped TSD density map of a 150-mm c-plane 4H-SiC wafer showing a reduced TSD density around at the edge of the facet region. Note: The scale bar was removed, and the heat map was generated with an arbitrary color scale due to confidentiality.

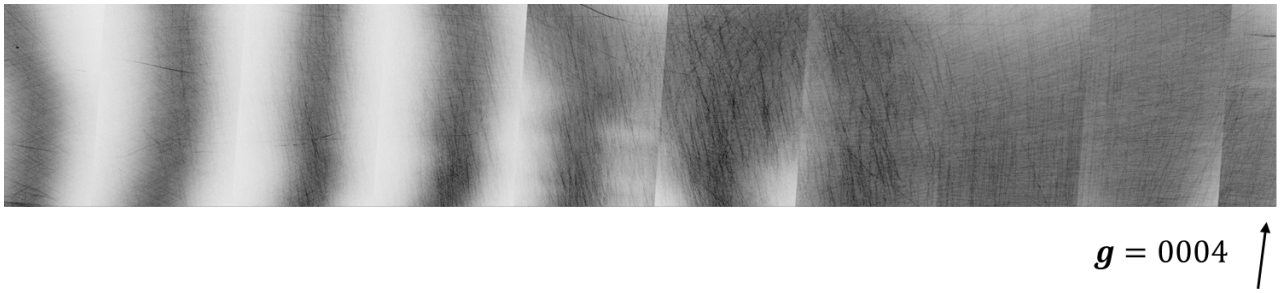

Fig. 3. Cropped overall XRT image *($E = 8.05keV, \boldsymbol{g} = 0004$)* of the axial sample to study the cause of TSD reduction at the facet boundary. Note: Contours on the left side of the image are caused by lattice bending effect. The scale bar was removed due to confidentiality.

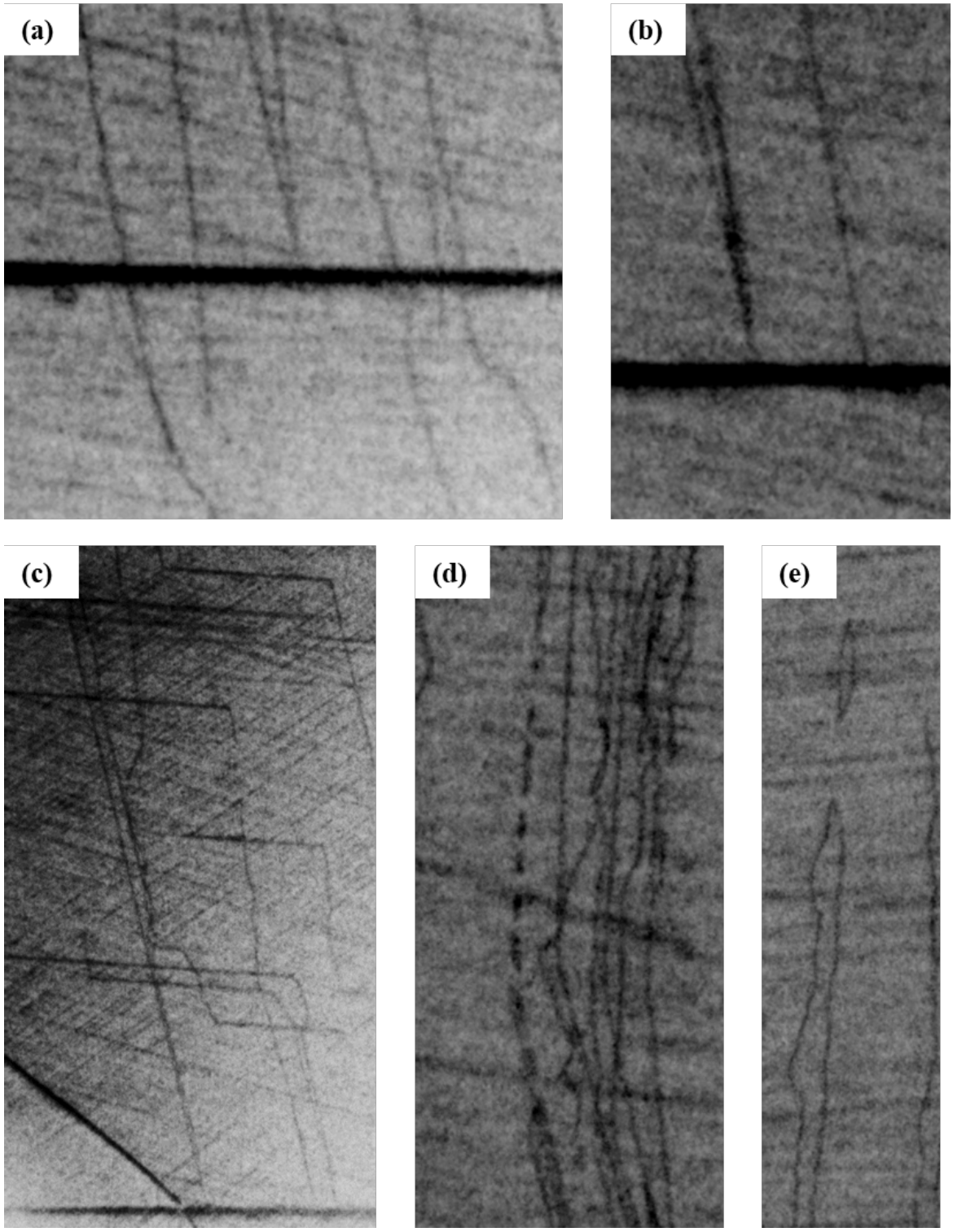

Fig. 4. Enlarged XRT images showing different dislocation behaviors of: (a) replication from the seed; (b) nucleation at the seed interface (dark horizontal linear contrast); (c) deflection; (d) climbing and (e) annihilation when dislocations with Burgers vectors of opposite signs meet. Note: The scale bar was removed due to confidentiality.

Fig. 5 shows two selected regions from the XRT image near the facet boundary. The facet boundary can be precisely depicted by an image from the scanner overlapping on the XRT image. From Fig. 5 (b) and (c), it can be observed that the TSDs inside the facet are strictly along c-direction. However, the TSDs outside the facet region tend to replicate towards other directions. Also, the change in the TSD orientations occurs precisely on the facet boundary. This is true for everywhere along the facet boundaries in this sample.

From this discovery, a schematic shown in Fig. 6 can be used to illustrate the cause of the reduction in TSD density at the facet boundary. It is known that a facet forms at a very early stage of PVT growth [8] due to a different growth rate along different directions. Step flow is the dominant mechanism outside the facet region, while spiral growth occurs mainly in the facet region. During crystal growth, the step flow direction is from the facet region to the rest of the crystal. This step flow can affect the propagation of TSDs so that the directions of TSDs bend towards the step flow direction, as shown in Fig. 6 (a). After a wafer is cut from the boule, the local TSD density at the facet boundary is lower than the nearby regions, shown in Fig. 6 (b). This mechanism is based on the XRT characterization and explains the direct cause of TSD reduction at the facet boundary.

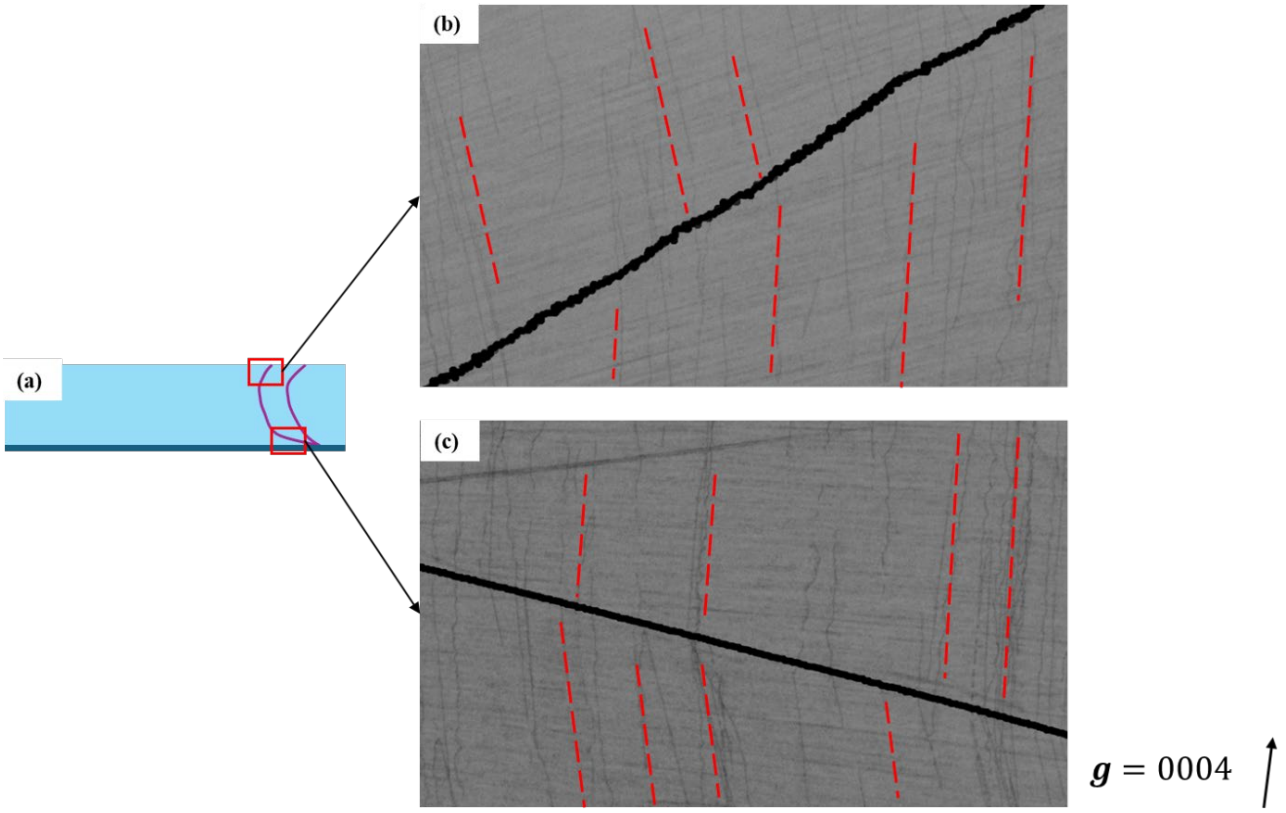

Fig. 5. (a) XRT images were magnified at two different positions on the sample near the facet boundary. (b) The facet boundary was denoted as dark line where the upper left is outside the facet and the lower right is inside the facet. (c) A similar image from another position in which the upper right is inside the facet and the lower left is outside the facet. Note: The scale bar was removed due to confidentiality.

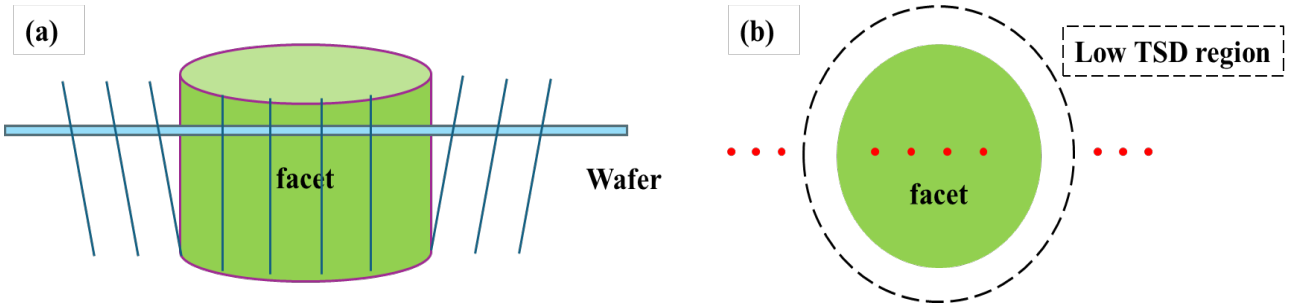

Fig. 6. A schematic showing the cause of TSD reduction at the facet boundary. (a) A perspective view of the region near the facet. (b) A top view of the wafer cut from the boule.

Elevated TSD Density in the Center of the Wafer. Fig. 7 shows a comparison between a production wafer and an engineering wafer with a consistent color scale. In Fig. 7 (b), elevated TSD density can be observed in the center of the wafer. To reveal the source of these TSDs, the same characterization work was done on an axial sample cut from the same boule. Fig. 8 is a magnified XRT image from the same region of the sample. In the red circles mark some 3-dimensional defect contrast spawning TSDs to the downstream of the crystal growth. However, no obvious cause of such defects can be seen in the same image.

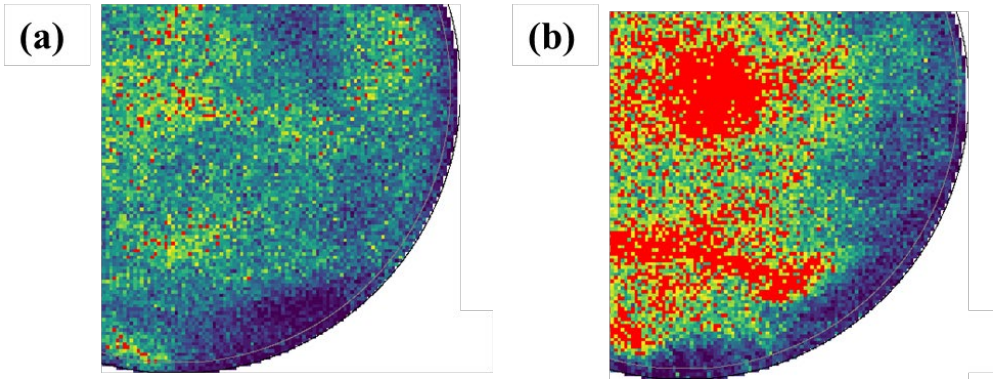

Fig. 7. Cropped TSD density maps of (a) a production 150-mm c-plane 4H-SiC wafer and (b) an engineering wafer showing elevated TSD density in the center. Note: The scale bar was removed, and the heat map was generated with an arbitrary color scale due to confidentiality.

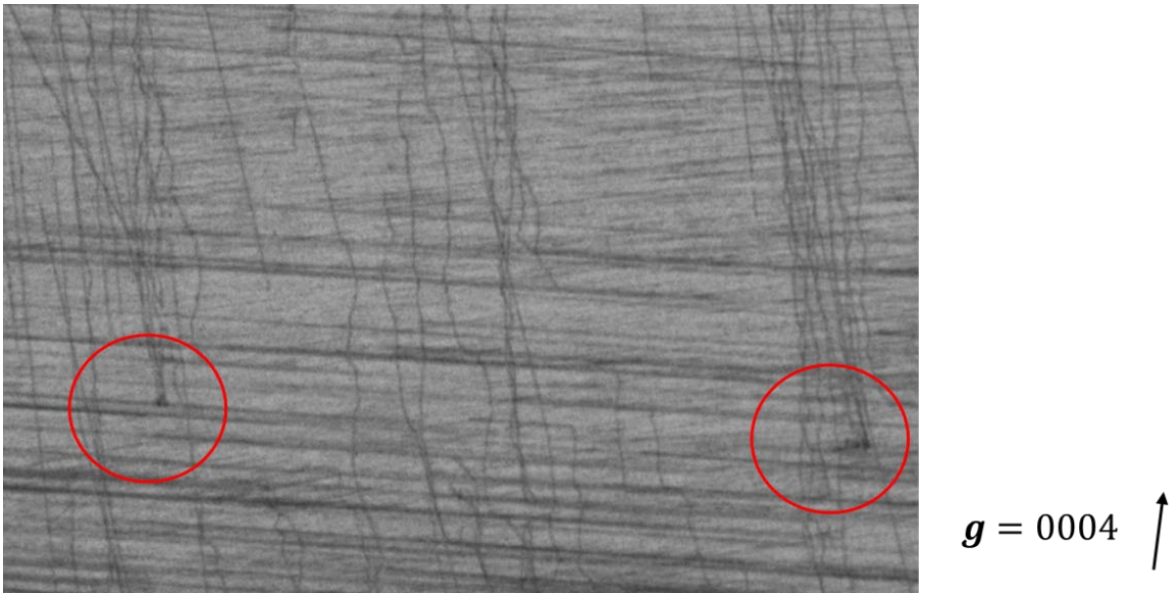

Fig. 8. Magnified XRT image taken from the middle region of the sample. Note: The scale bar was removed due to confidentiality.

To confirm the structure of the 3-dimensional defects in the XRT image, optical microscopy (OM), scanning electron microscopy (SEM) and focused ion beam (FIB) were employed. Fig. 9 (a) is an OM image showing hexagonal shapes of the defect on a c-plane wafer with high TSD density in the middle region. For a more detailed view, Fig. 9 (b) shows the SEM image of one of the hexagonal shapes. It is confirmed that such 3-dimensional features have void structures with the size of around 100 μm. Furthermore, Fig. 9 (d) shows the cross-sectional view of the void by imaging the sample prepared by FIB at the location shown in Fig. 9 (c). It is found that the void defect started from a smaller size and developed larger before being overgrown.

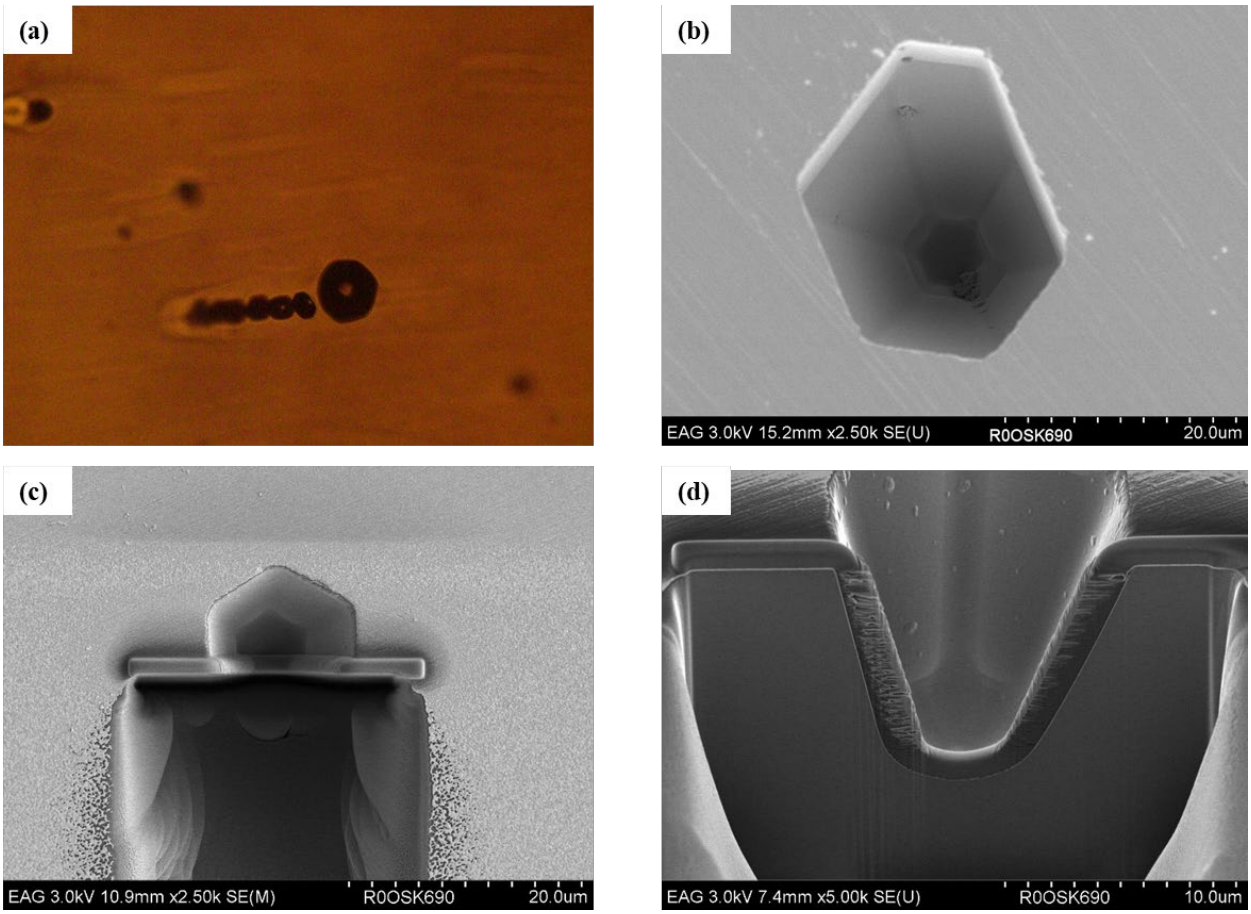

Fig. 9. (a) Optical microscopic image of hexagonal shaped defects observed in a c-plane wafer with high TSD density in the middle. (b) SEM image of the 3D feature showing a void structure with a size around 100 μm. (c) The location of FIB analysis conducted on the void structure. (d) The cross-sectional view of the void structure.

Several studies have been conducted on the void defects in SiC crystals. One study [11] has indicated that when a void forms on top of a micropipe, the micropipe can be dissociated into multiple TSDs after the void is overgrown. Together with another study [12], it has been shown that the void can be originated and transported from the backside of the seed crystal. A recent study [13] has indicated that the improper seed mounting can be the root cause of the formation of hexagonal voids. However, observations in these studies were not made in this sample. While further analysis on this sample is in progress, the formation mechanism of such void defects in this study remains unclear.

Summary

In this paper, Lab-based XRT was demonstrated to be a useful characterization method on axial samples from SiC boules grown by PVT method. Dislocation behaviors during crystal growth can be observed, and explanations of the change in dislocation density in SiC substrate wafers can be made. It is found that the change in TSD propagation direction at the facet boundary, which is affected by the step flow direction, is the direct cause of reduced TSD density near the facet region. It is also found that void defects are responsible for the elevated TSD density in the center of some wafers. However, some key observations from previous studies are not made to confirm the void formation mechanism, which is still under investigation.

References

[1] B. Raghothamachar, M. Dudley, X-Ray Topography, Materials Characterization, ASM International 2019.

[2] T. Ailihumaer, H. Peng, Y. Liu, B. Raghothamachar, M. Dudley, Characterization of Dislocations in 4H-SiC Single Crystals at the Initial Growth Stage by Synchrotron X-ray Topography, ECS Transactions 98(6) (2020) 125.

[3] Q. Cheng, T. Ailihumaer, H. Peng, Y. Liu, B. Raghothamachar, M. Dudley, Analysis of Dislocations in PVT-Grown 6H-SiC through Grazing-Incidence X-Ray Topographic Images and Ray-Tracing Simulation, ECS Transactions 98(6) (2020) 133.

[4] H. Peng, Y. Liu, T. Ailihumaer, B. Raghothamachar, M. Dudley, K. Sampayan, S. Sampayan, Investigation of Dislocations in 6H-SiC Axial Samples Using Synchrotron X-Ray Topography and Ray Tracing Simulation, ECS Transactions 104(7) (2021) 147-155.

[5] Q.Y. Cheng, H.Y. Peng, S.S. Hu, Z.Y. Chen, Y.F. Liu, B. Raghothamachar, M. Dudley, Ray-Tracing Simulation Analysis of Effective Penetration Depths on Grazing Incidence Synchrotron X-Ray Topographic Images of Basal Plane Dislocations in 4H-SiC Wafers, Materials Science Forum, Trans Tech Publ, 2022, pp. 366-370.

[6] H. Peng, Y. Liu, Z. Chen, Q. Cheng, S. Hu, B. Raghothamachar, M. Dudley, K. Sampayan, S. Sampayan, Synchrotron X-ray topographic characterization of dislocations in 6H-SiC axial samples, Journal of Crystal Growth 579 (2022) 126459.

[7] Z. Chen, Y. Liu, Q. Cheng, S. Hu, B. Raghothamachar, M. Dudley, Analysis of strain in ion implanted 4H-SiC by fringes observed in synchrotron X-ray topography, Journal of Crystal Growth 627 (2024) 127535.

[8] S. Hu, Y. Liu, Q. Cheng, Z. Chen, X. Tong, B. Raghothamachar, M. Dudley, Investigation of defect formation at the early stage of PVT-grown 4H-SiC crystals, Journal of Crystal Growth 628 (2024) 127542.

[9] G. Dhanaraj, B. Raghothamachar, M. Dudley, Growth and Characterization of Silicon Carbide Crystals, in: G. Dhanaraj, K. Byrappa, V. Prasad, M. Dudley (Eds.), Springer handbook of crystal growth, Springer Science & Business Media 2010, p. 797.

[10] F.Z. Wu, H.H. Wang, S.Y. Byrapa, B. Raghothamachar, M. Dudley, E. Sanchez, D.M. Hansen, R. Drachev, S.G. Mueller, M.J. Loboda, Synchrotron X-ray Topography Studies of the Propagation and Post-Growth Mutual Interaction of Threading Growth Dislocations with c-component of Burgers Vector in PVT-Grown 4H-SiC, Materials Science Forum, Trans Tech Publ, 2012, pp. 343-346.

[11] T.A. Kuhr, E.K. Sanchez, M. Skowronski, W.M. Vetter, M. Dudley, Hexagonal voids and the formation of micropipes during SiC sublimation growth, Journal of Applied Physics 89(8) (2001) 4625-4630.

[12] T. Fujimoto, H. Tsuge, M. Katsuno, S. Sato, H. Yashiro, H. Hirano, T. Yano, A possible mechanism for hexagonal void movement observed during sublimation growth of SiC single crystals, Materials Science Forum, Trans Tech Publ, 2013, pp. 577-580.

[13] A. Arora, A. Patel, B.S. Yadav, A. Goyal, O.P. Thakur, A.K. Garg, R. Raman, Study on evolution of micropipes from hexagonal voids in 4H-SiC crystals by cathodoluminescence imaging, Microscopy and Microanalysis 27(1) (2021) 215-226.